

# Two Competing Linear Models for Flexible Robots: Comparison, Experimental Validation, and Refinement

Ryan Krauss, Olivier Brüls and Wayne Book

**Abstract**—The modeling of a rigid robot attached to a flexible base is addressed in this work. Two approaches are compared: the Finite Element Method (FEM) and the Transfer Matrix Method (TMM). Initially, idealized models of the hydraulic actuators are used that do not include flexible effects in the joints. Those models greatly overestimate the second natural frequency of the system, therefore the identification of local flexibilities in the joints is pursued to improve the results. The very good agreement between both approaches, and their ability to represent the physical system (once joint flexibility is included), confirms their efficiency and relevance in this context.

## I. INTRODUCTION

This work compares two competing approaches for modeling flexible robots: the transfer matrix method (TMM) and the finite element method (FEM) with a reduction technique. Initial models are developed based only on information that should be available before the construction of the robot (basically geometry and material properties). Valuable insights result from comparing these models to one another and to experiments. First, the two approaches give very similar results and validate one another. Second, a comparison with experimental results calls for a refinement of those initial models. In particular, a more realistic actuator model and flexible effects in the joints must be included. Two methods for experimentally determining the parameters of the refined model are proposed and compared.

SAMII, a rigid robot on the end of a long, flexible beam is used as a test case. The system is shown in Fig. 1. The rigid robot has six hydraulically actuated links. Digital optical encoders and potentiometers measure the joint positions and the vibration is measured with piezoelectric accelerometers  $a_0$ ,  $a_1$  and  $a_2$ .

Linear models are built for small motions around a reference configuration where all the links are vertically aligned. Only joints 2 and 3 excite vibration in the  $xy$ -vertical plane. All other joints are considered locked.

## II. MODELING OF FLEXIBLE MECHANISMS: STATE OF THE ART

In order to design the control system of a mechanism with significant flexibilities, a relevant model of its dynamic

R. Krauss is with the George W. Woodruff School of Mechanical Engineering, Georgia Institute of Technology, Atlanta, GA 30332, USA [gtg708j@mail.gatech.edu](mailto:gtg708j@mail.gatech.edu)

O. Brüls is with the Department of Aerospace, Mechanics and Material Science, University of Liège, Belgium [o.bruls@ulg.ac.be](mailto:o.bruls@ulg.ac.be)

W. Book is the Husco/Ramirez Distinguished Chair in Fluid Power and Motion Control in the George W. Woodruff School of Mechanical Engineering, Georgia Institute of Technology, Atlanta, GA 30332, USA [wayne.book@me.gatech.edu](mailto:wayne.book@me.gatech.edu)

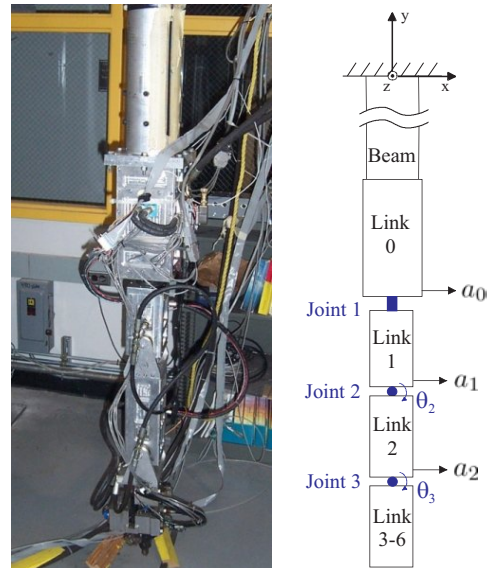


Fig. 1. SAMII test-bed and mechanical topology.

behavior is desirable. Three conflicting requirements should be satisfied: accuracy in the bandwidth of the controller, low-order, and closed-form expression. This section briefly reviews modeling methods for flexible multi-body systems. We make a first distinction between the methods working directly with distributed parameters, such as the transfer matrix method, and the methods based on a discretized parameterization, such as the finite element method.

### A. The Transfer Matrix Method (TMM)

The transfer matrix method deals with the spatial differential equations directly, without requiring discretization. Therefore the method is able to give exact natural frequencies and mode shapes and retains infinite bandwidth.

To understand what is meant by this, consider a beam element. The states of a beam are related by

$$\frac{dV}{dx} = -\mu\omega^2 w, \quad \psi = -\frac{dw}{dx}, \quad \text{and} \quad M = EI \frac{d\psi}{dx} \quad (1)$$

where  $V$  is the shear force,  $w$  is the lateral displacement,  $\psi$  is the angular displacement,  $M$  is the bending moment,  $E$  is the modulus of elasticity,  $I$  is the second moment of inertia, and  $\mu$  is the mass per unit length.  $\omega$  is the driving frequency.

A solution for the shear force is assumed in the form

$$V = A_1 Ch_\gamma + A_2 Sh_\gamma + A_3 C_\gamma + A_4 S_\gamma \quad (2)$$

where  $\beta^4 = \omega^2 l^4 \mu / EI$ ,  $\gamma = \beta x / l$ ,  $S_\gamma = \sin(\gamma)$ ,  $C_\gamma = \cos(\gamma)$ ,  $Sh_\gamma = \sinh(\gamma)$ ,  $Ch_\gamma = \cosh(\gamma)$ , and  $l$  is the length of the beam. A solution for all four states can then be written as

$$\mathbf{z}(x) = \mathbf{B}(x)\mathbf{A} \quad (3)$$

where

$$\mathbf{B} = \begin{bmatrix} a l S h_\gamma / \beta^3 & a l C h_\gamma / \beta^3 & -a l S_\gamma / \beta^3 & a l C_\gamma / \beta^3 \\ a C h_\gamma / \beta^2 & a S h_\gamma / \beta^2 & -a C_\gamma / \beta^2 & -a S_\gamma / \beta^2 \\ l S h_\gamma / \beta & l C h_\gamma / \beta & l S_\gamma / \beta & -l C_\gamma / \beta \\ C h_\gamma & S h_\gamma & C_\gamma & S_\gamma \end{bmatrix} \quad (4)$$

$$\mathbf{z} = \begin{bmatrix} -w \\ \psi \\ M \\ V \end{bmatrix}, \quad \mathbf{A} = \begin{bmatrix} A_1 \\ A_2 \\ A_3 \\ A_4 \end{bmatrix}, \quad \text{and} \quad a = \frac{l^2}{EI} \quad (5)$$

The states at each end of the beam could be written as

$$\mathbf{z}(0) = \mathbf{B}(0)\mathbf{A} \quad \text{and} \quad \mathbf{z}(L) = \mathbf{B}(L)\mathbf{A} \quad (6)$$

$\mathbf{B}(0)$  and  $\mathbf{B}(L)$  refer to substituting  $x = 0$  or  $x = L$  into the expression for  $\gamma$  used in eqn. 4). Solving the first of eqn. 6 for  $\mathbf{A}$  gives

$$\mathbf{A} = [\mathbf{B}(0)]^{-1} \mathbf{z}(0) \quad (7)$$

Substituting this expression into the second of eqn. 6 gives

$$\mathbf{z}(L) = \mathbf{B}(L) [\mathbf{B}(0)]^{-1} \mathbf{z}(0) \quad (8)$$

so that a transfer matrix for a beam element can be written as

$$\mathbf{U}_{beam} = \mathbf{B}(L) [\mathbf{B}(0)]^{-1} \quad (9)$$

Note that this transfer matrix transfers the state vector from one end of the beam to the other and that no discretization is necessary.

An in depth explanation of the transfer matrix method can be found in [1]. An introduction tailored specifically to flexible robotics can be found in chapter 22 of [2].

The transfer matrix method (TMM) is a technique for modeling linear, interconnected bodies. It is particularly well suited to modeling of serially connected systems (systems with branches may also be modeled, but with some additional complications). Each element of the system is represented by a matrix which transfers a vector of states from one end of the element to the other. Serial connection is handled through multiplication of the matrices representing the individual bodies, producing a transfer matrix for the entire system. One strength of the method is that intermediate boundary conditions at the connections of the elements are handled automatically and exactly. The natural frequencies of the system are determined by finding the value of the frequency variable which causes a sub-determinant of the overall system transfer matrix to equal zero.

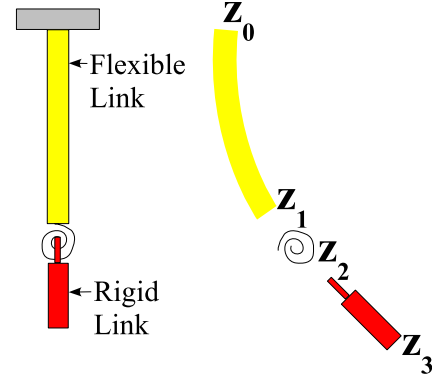


Fig. 2. Transfer matrix example system.

As an example, consider a robot made up of one flexible link, a flexible joint, and a rigid link. Such a system is shown in Fig. 2. The system could be modeled with 4 state vectors ( $\mathbf{z}_0 - \mathbf{z}_3$ ).

If the flexible joint is modeled as a torsional spring, an appropriate transfer matrix for this element would be

$$\mathbf{K} = \begin{bmatrix} 1 & 0 & 0 & 0 \\ 0 & 1 & 1/k & 0 \\ 0 & 0 & 1 & 0 \\ 0 & 0 & 0 & 1 \end{bmatrix}. \quad (10)$$

The transfer matrix for the flexible beam would be that given by eqn. 9.

A transfer matrix for the rigid link could be derived based on its equations of motion [3] and a model for the complete system could be written as

$$\mathbf{z}_3 = \mathbf{R}\mathbf{K}\mathbf{U}_{beam}\mathbf{z}_0 \quad (11)$$

where  $\mathbf{R}$  is the transfer matrix of the rigid link.

### B. Methods based on a Spatial Discretization (FEM)

In contrast with the TMM, methods based on spatial discretization are only able to describe the dominant dynamic behavior of the original infinite-dimensional system. Different methods may be classified according to their generality and computational efficiency. On the one hand, assumed-modes based methods [4], [5] can exploit recursive and/or symbolic formulations in order to build compact and efficient models for mechanisms with simple topologies. On the other hand, the finite element method is systematic and able to model accurately complex flexible mechanisms.

For instance, the FEM formulation proposed by Géradin and Cardona [6] is a very powerful tool for the analysis of flexible mechanisms with large displacements, rotations and deformations. The spatial discretization involves a high number of nodal degrees of freedom (d.o.f.s) interrelated by kinematic constraints. The equations of motion have the form

$$\begin{cases} \mathbf{M} \ddot{\mathbf{q}} + \Phi_{\mathbf{q}}^T \lambda - \mathbf{g}(\mathbf{q}, \dot{\mathbf{q}}) = \mathbf{0} \\ \Phi(\mathbf{q}) = \mathbf{0} \end{cases} \quad (12)$$

where  $\mathbf{q}$  denotes the vector of the initial FEM coordinates,  $\boldsymbol{\lambda}$  is the vector of Lagrange multipliers,  $\mathbf{M}$  is the mass matrix,  $\mathbf{g}$  is the vector of apparent forces (*i.e.* external forces, internal forces and complementary inertia forces),  $\Phi$  is the set of kinematic constraints and  $\Phi_{\mathbf{q}}$  is the constraint gradient.

The treatment of this high-order set of nonlinear equations involves expensive computations. Hence, the component-mode technique can be exploited to simplify the model with a limited loss in accuracy [7]. This method is based on a modal analysis of the linearized equations around a configuration (a generalization has been proposed by Brüls *et al.* [8] to represent the nonlinear dependence with respect to the mechanical configuration). The modal parameterization involves a small number of rigid modes and flexible modes:

$$\mathbf{q} = \underbrace{\begin{bmatrix} \phi_r & \phi_f \end{bmatrix}}_{=\phi} \underbrace{\begin{bmatrix} \theta \\ \eta_f \end{bmatrix}}_{=\eta} \quad (13)$$

The rigid modes  $\phi_r$  are defined with respect to the actuator d.o.f.s.  $\theta$ , and the flexible modes  $\phi_f$  are associated with additional modal coordinates  $\eta_f$ . The rigid and flexible modes represent the motion of the *whole* mechanism, including the joints and rigid bodies. This is a conceptual difference with the super-element technique [9], where the component-modes are associated with isolated flexible links.

The number of flexible modes is selected by the user in order to get the required compromise between complexity and accuracy. The reduced equations of motion follow from classical transformation relations:

$$\underbrace{\begin{bmatrix} \bar{\mathbf{M}}_{rr} & \bar{\mathbf{M}}_{rf} \\ \bar{\mathbf{M}}_{fr} & \bar{\mathbf{M}}_{ff} \end{bmatrix}}_{=\bar{\mathbf{M}}} \begin{bmatrix} \ddot{\boldsymbol{\theta}} \\ \ddot{\boldsymbol{\eta}}_f \end{bmatrix} + \underbrace{\begin{bmatrix} \mathbf{0} & \mathbf{0} \\ \mathbf{0} & \bar{\mathbf{K}}_{ff} \end{bmatrix}}_{=\bar{\mathbf{K}}} \begin{bmatrix} \boldsymbol{\theta} \\ \boldsymbol{\eta}_f \end{bmatrix} = \begin{bmatrix} \mathbf{T} \\ \mathbf{0} \end{bmatrix} \quad (14)$$

where  $\bar{\mathbf{M}}$  is the reduced mass matrix,  $\bar{\mathbf{K}}$  is the reduced stiffness matrix and  $\mathbf{T}$  is the vector of actuator forces.

### III. MODEL WITH PERFECT JOINTS

#### A. Initial Assumptions

In order to model the dynamics excited by the control voltage, a model of the hydraulic actuators of the rigid robot should be included. Initially, those actuators are modeled as perfect velocity sources with no flexibility, which means that the joint angular velocity  $\dot{\theta}$  is proportional to the voltage  $v$ :

$$\dot{\theta} = g_a v \quad (15)$$

where  $g_a$  is a constant gain.

#### B. TMM Model

If locked joints are assumed to have no flexibility, a transfer matrix model of the idealized system would be

$$\mathbf{z}_{tip} = \mathbf{R}_{3-6} \mathbf{R}_2 \mathbf{R}_1 \mathbf{R}_0 \mathbf{B} \mathbf{z}_{base} \quad (16)$$

TABLE I  
NATURAL FREQUENCIES (Hz)

Experiments	TMM	FEM
1.7	2.299	2.298
7.4	21.417	21.412

where  $\mathbf{B}$  is the transfer matrix of the beam (the flexible base),  $\mathbf{R}_0$ - $\mathbf{R}_2$  represent the rigid links 0-2, and  $\mathbf{R}_{3-6}$  represents rigid links 3-6 lumped together.  $\mathbf{z}_{base}$  and  $\mathbf{z}_{tip}$  represent the state vectors at the base and tip of the entire system. Because the boundary conditions are clamped at the base and free at the tip:

$$\mathbf{z}_{base} = \begin{bmatrix} 0 \\ 0 \\ M_{base} \\ V_{base} \end{bmatrix} \quad \text{and} \quad \mathbf{z}_{tip} = \begin{bmatrix} -w_{tip} \\ \psi_{tip} \\ 0 \\ 0 \end{bmatrix} \quad (17)$$

#### C. Reduced FEM Model

The flexible beam is modeled using 15 finite elements, and 89 degrees of freedom are involved in the initial FEM model. In the reduced model, two rigid modes are associated with  $\theta_2$  and  $\theta_3$ , and four flexible modes are retained from the component-mode synthesis ( $\dim \eta = 6$ ).

A small Rayleigh damping is assumed, which means that a damping matrix  $\bar{\mathbf{C}} = \alpha \bar{\mathbf{K}} + \beta \bar{\mathbf{M}}$  is introduced in the linear model.

#### D. Comparison of the Results

The natural frequencies associated with both models are compared in Table I: the two methods validate one another, but there is considerable discrepancy with the experimental results.

#### E. Shortcomings of the Model with Perfect Joints

The model with perfect joints does not adequately capture the dynamics of the physical system in two ways. The first is that the predicted natural frequencies are too high, especially for the second mode (see Table I). The second shortcoming is that the actuator is not a perfect velocity source near the second natural frequency of the system. This can be seen in the actuator Bode plot at around 7.2Hz (Fig. 3).

Two improvements to the actuator model are considered to overcome these shortcomings. The first is to include velocity feedback in the actuator model. The second is to incorporate joint flexibility. Determining the parameters of the enhanced model requires an experimental identification procedure, which is also described in the next section.

### IV. REFINEMENT OF THE INITIAL MODEL

#### A. An Actuator Model with Intrinsic Velocity Feedback

In order to account for the intrinsic velocity feedback that regulates the flow through the valve of a hydraulic actuator, the following actuator model is proposed:

$$T = g_v (g_a v - \dot{\theta}) \quad (18)$$

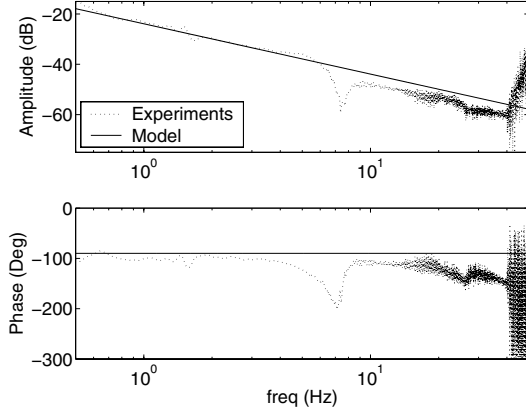


Fig. 3. Transfer function of Actuator 2. Input =  $v_2$  and output =  $\theta_2$

where  $T$  is the torque applied by the actuator,  $v$  is the voltage to the actuator,  $\dot{\theta}$  is the angular velocity of the joint, and  $g_v$  and  $g_a$  are constants to be determined.

If  $g_v \rightarrow \infty$ , this model is equivalent to the velocity source model. For finite  $g_v$ , the transfer function between  $v$  and  $\theta$  is affected by the plant dynamics near the resonances.

Tuning the value of  $g_v$  modifies the damping in the closed-loop system, but the natural frequencies remain almost unaffected. This means that intrinsic velocity feedback may explain why the actuator differs from a pure velocity source, but it does not explain why the predicted natural frequencies are too high. An investigation into unmodeled flexibility addresses this problem.

### B. Joint Flexibilities

The connections between the various bodies of the mechanical system are never perfectly rigid. This effect can be modeled considering lumped stiffnesses at different levels:  $k_{clamp}$  is the stiffness associated with the clamping of the beam to its support,  $k_{J1}$  is the stiffness of joint 1,  $k_{a2}$  and  $k_{a3}$  are the stiffnesses in the active joints. Fig. 4 shows a possible model of flexibility in an actuated joint. It is not clear whether  $\theta_s$ , the angle measured by the sensors, corresponds to  $\theta_a$ , the actuator angle (collocated configuration), or to  $\theta$ , the link angle (non-collocated configuration); both cases will be considered.

Two methods for identifying the parameters of the refined model are considered in the following. Method 1 uses data taken with the robot in the initial configuration shown in Fig. 1. Method 2 seeks to isolate the joint flexibility by adding braces that remove the dynamics of the flexible beam. In both cases, the mechanism is excited by joint 2, and measurements are realized with the joint encoders and extra accelerometers.

### C. Identification Method 1: Initial Configuration

Several parameters have to be identified:

- $k_{clamp}$ ,  $k_{J1}$ ,  $k_{a2}$  and  $k_{a3}$  are the local stiffnesses, which have a dominant influence on the natural fre-

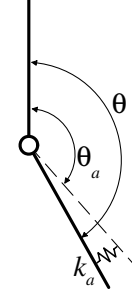


Fig. 4. Flexibility in the actuated joints.  $\theta$  is the angle between the rigid links,  $\theta_a$  is the angular displacement of the actuator,  $k_a$  is the equivalent stiffness, which can be associated with the transmission mechanism.

TABLE II

SUMMARY OF IDENTIFIED PARAMETERS FROM THE METHODS DISCUSSED IN SECTIONS IV-C & IV-D (SI UNITS).

	Method 1	Method 2
$k_{clamp}$	2.674e5	–
$k_{J1}$	0.136e5	0.0651e5
$k_{a2}$	0.108e5	0.0713e5
$k_{a3}$	0.252e5	–
$g_{v2}$	500	–
$g_{v3}$	150	–

quencies and the zeros of the whole mechanical system;

- $g_{v2}$  and  $g_{v3}$  are the actuator gains, which mainly influence the damping in the closed-loop system.

In order to exploit this uncoupling between parameters that affect the natural frequencies and those that affect damping, a two-stage optimization technique is applied:

- 1) Establishment of the stiffness parameters minimizing a quadratic error function:

$$e = \sum_{i=1}^2 \left( \frac{f_{i,exp} - f_{i,model}}{f_{i,exp}} \right)^2 + \left( \frac{z_{1,exp} - z_{1,model}}{z_{1,exp}} \right)^2$$

where  $f_i$  ( $i = 1, 2$ ) are the first two natural frequencies and  $z_1$  is the first zero of the transfer function from  $\theta_2$  to  $a_0$  (link 0 acceleration). This minimization is based on an automatic optimization routine (Nelder-Mead algorithm).

- 2) Adjustment of  $g_{vi}$  in order to fit the amplitudes in the transfer function  $v_i/\theta_i$ ,  $i = 2, 3$ .

We have tested this optimization for both the collocated and non-collocated cases. In the second case, good agreement could not be obtained between the experiment and the model. Therefore, we conclude that the actuators and sensors are actually collocated. For the collocated case, the parameters resulting from the optimization are summarized in Table II.

The comparison between the model and the experimental results is presented in Figs. 5 and 6. The natural frequencies of the model are given in Table III, and the discrepancies have almost disappeared at this level.

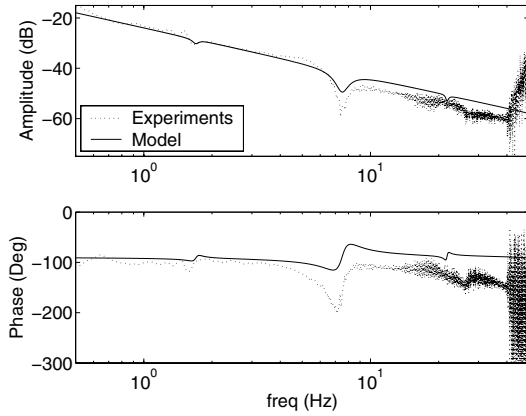


Fig. 5. Optimized transfer function,  $v_2$  to  $\theta_2$ .

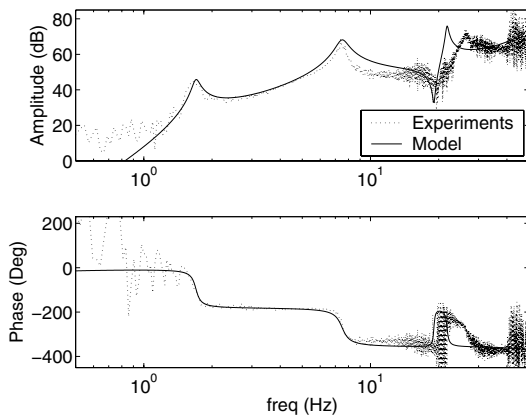


Fig. 6. Optimized transfer function,  $\theta_2$  to  $a_0$ .

In order to validate the identified parameters, a second identification was conducted.

#### D. Identification Method 2: Bracing the System

In an attempt to isolate the joint dynamics from the base flexibility, SAMII's base was braced to the floor as seen in Fig. 7. Testing in this configuration emphasizes the need to include the flexibility of joints 1 & 2 in the models.

The effective torsional stiffnesses of joints 1 & 2 are estimated by a minimization routine whose cost function is

$$e = (f_{1,exp}^* - f_{1,model}^*)^2 + w \left( \frac{\phi_{1,exp}^*(1)}{\phi_{1,exp}^*(2)} - \frac{\phi_{1,model}^*(1)}{\phi_{1,model}^*(2)} \right)^2 \quad (19)$$

TABLE III  
NATURAL FREQUENCIES OF THE REFINED MODELS (Hz)

Experiments	Model (1)	Model (2)
1.7	1.703	2.2
7.4	7.394	6.0



Fig. 7. SAMII with braces attached to the base.

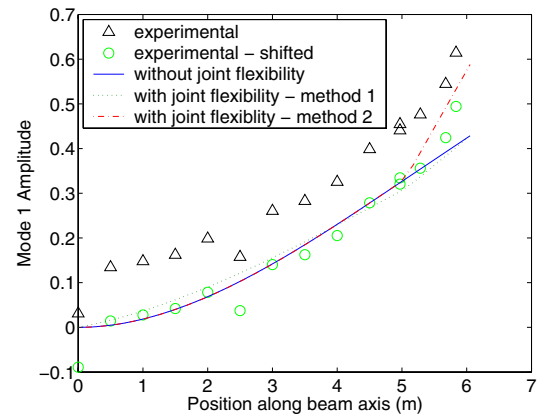


Fig. 8. Overlay of first mode shapes from the models and experiment (experimental data has been shifted to remove an offset).

where  $f_1^*$  is the first natural frequency of the braced mechanism,  $\phi_1^*(i)$  is the value of the corresponding mode shape at accelerometer location  $i$  ( $i = 1, 2$ ), and  $w$  is a weighting factor to set the relative importance of these two errors.

The outputs of this optimization are torsional spring constants for joints 1 & 2. These estimates are compared with those from the method of section IV-C in Table II: while the orders of magnitude are consistent, the first method is superior in predicting the natural frequencies.

The natural frequencies given by this method are presented in the last column of Table III.

#### E. Mode Shape Comparison

Mode shapes from models with and without flexibility in the joints are shown in Fig. 8-9. The experimental data for mode 1 seems to have an offset, so the data is also plotted with a constant subtracted from it. The distinct slope changes at joints 1 & 2 are correctly predicted by the models that account for the local flexibilities in the joints.

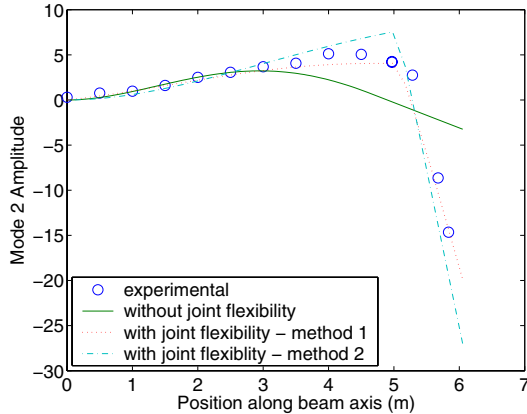


Fig. 9. Overlay of second mode shapes from the models and experiment.

## V. FEM AND TMM: COMPARISON

The transfer matrix method and the finite element method give very similar results in the particular case considered here. Both models have more or less the same level of accuracy. In a more global framework, each method has its advantages and disadvantages which deserve a few qualitative comments. The following comparison concerns the generality of each formulation and the effort required to build the model.

### A. Generality

The major advantage of the FEM is its generality: nonlinear models can be established for flexible mechanisms with arbitrarily complex geometries and large amplitude motion. The TMM is best suited for simple geometries such as beams and rigid links and linear models around nominal configurations of the system.

The actuator model discussed in section IV-A and used to generate Fig. 5 was implemented using the FEM. Implementing this exact model with the TMM is difficult because of differences in formulation. A Bode plot similar to Fig. 5 can be generated using the TMM by modeling the actuator as an angular velocity source in series with a torsional damper.

### B. Model construction effort

The computational load required to build the models is another interesting issue. The TMM naturally leads to small matrices (4x4 in the case considered here), but these matrices contain transcendental equations. The main computational effort is spent in the numerical search algorithm for the natural frequencies, which are roots of these transcendental equations.

In contrast, the FEM leads to large matrices, but they are sparse and numerical techniques for dealing with them are well developed. Further, the cost to manipulate a high-order FEM model depends on the spatial discretization level. Component-mode techniques can be efficiently exploited to construct a reduced model from an initial FEM model; leading to an adjustable compromise between accuracy and

complexity (this method can be extended for mechanisms with significant configuration changes [8]).

Concerning the programming effort, a drawback of the FEM comes from the complexity of the formulation. Hopefully, commercial software are widely available with powerful graphical interfaces and drivers to software used in control engineering, such as Matlab. For these reasons, they can be used even by non-specialists in computational mechanics. On the other hand, using the TMM requires the writing of subroutines for each matrix type in Matlab or some other language well suited to linear algebra and root finding. So, in some sense, no commercial software is required. Once subroutines for the various matrices exist, model construction using the TMM is straight forward.

## VI. CONCLUSIONS

The transfer matrix method and the finite element method with a reduction procedure have been shown to produce very similar models for a robot with flexible links and flexible joints. When joint flexibility is accounted for, the agreement between these models and experimental results is fairly good.

## VII. ACKNOWLEDGMENTS

O. Brüls is supported by a grant from the Belgian National Fund for Scientific Research (FNRS) which is gratefully acknowledged. This work also presents research results of the Belgian programme on Inter-University Poles of Attraction initiated by the Belgian state, Prime Minister's office, Science Policy Programming. The scientific responsibility is assumed by its authors.

R. Krauss gratefully acknowledges the support of the Fluid Power and Motion Control Center.

## REFERENCES

- [1] E. C. Pestel and F. A. Leckie, *Matrix Methods in Elastomechanics*. New York, NY: McGraw-Hill, 1963.
- [2] T. R. Kurfess, *Robotics and Automation Handbook*. Boca Raton, FL: CRC Press, 2004.
- [3] W. J. Book, "Modeling, design, and control of flexible manipulator arms," Ph.D. dissertation, Massachusetts Institute of Technology, Department of Mechanical Engineering, Apr. 1974.
- [4] W. Book, "Recursive Lagrangian Dynamics of Flexible Manipulator Arms," *Int. Jnl. of Robotics Research*, vol. 3, no. 3, pp. 87–101, 1984.
- [5] S. Cetinkunt and W. Book, "Symbolic modeling and dynamic simulation of robotic manipulators with compliant links and joints," *Robotics and Computer-Integrated Manufacturing*, vol. 5, no. 4, pp. 301–310, 1989.
- [6] M. Géradin and A. Cardona, *Flexible Multibody Dynamics: A Finite Element Approach*. New York: John Wiley & Sons, 2001.
- [7] W. Hurty, "Dynamic analysis of structural systems using component modes," *AIAA Jnl.*, vol. 3, no. 4, pp. 678–685, 1965.
- [8] O. Brüls, P. Duysinx, and J.-C. Golinval, "Generation of closed-form models for the control of flexible mechanisms: a numerical approach," in *Proc. of the 7th Int. Conf. on Motion and Vibration Control (MOVIC)*, Saint-Louis, United States, August 2004.
- [9] A. Shabana and R. Wehage, "A coordinate reduction technique for dynamic analysis of spatial substructures with large angular rotations," *J. Struct. Mech.*, vol. 11, pp. 401–431, 1983.